TOXICOLOGICAL SCIENCES **119(2)**, 308–318 (2011)
doi:10.1093/toxsci/kfq326
Advance Access publication October 21, 2010

Determining Epidermal Disposition Kinetics for Use in an Integrated Nonanimal Approach to Skin Sensitization Risk Assessment

Michael Davies,*[,1] Ruth U. Pendlington,* Leanne Page,† Clive S. Roper,† David J. Sanders,* Clare Bourner,* Camilla K. Pease,* and Cameron MacKay*

*Safety and Environmental Assurance Centre, Sharnbrook, Bedford MK44 1LQ, UK; and †In Vitro Sciences, Charles River, Tranent, Edinburgh EH33 2NE, UK

[1]To whom correspondence should be addressed at Safety and Environmental Assurance Centre, Unilever, Colworth Science Park, Sharnbrook, Bedford MK44 1LQ, UK. Fax: +44-1234-222632. E-mail: michael.davies@unilever.com.

Received August 27, 2010; accepted October 13, 2010

Development of risk assessment methods for skin sensitization in the absence of toxicological data generated in animals represents a major scientific and technical challenge. The first step in human skin sensitization induction is the transport of sensitizer from the applied dose on the skin surface to the epidermis, where innate immune activation occurs. Building on the previous development of a time course *in vitro* human skin permeation assay, new kinetic data for 10 sensitizers and 2 nonsensitizers are reported. Multicompartmental modeling has been applied to analyze the data and determine candidate dose parameters for use in integrated risk assessment methods: the area under the curve (AUC) and maximum concentration (C_{max}) in the epidermis. A model with two skin compartments, representing the stratum corneum and viable skin (epidermis and dermis), was chosen following a formal model selection process. Estimates of the uncertainty, as well as average values of the epidermal disposition kinetics parameters, were made by fitting to the time course skin permeation data from individual skin donors. A potential reduced time course method is proposed based on two time points at 4 and 24 h, which gives results close to those from the full time course for the current data sets. The time course data presented in this work have been provided as a resource for development of predictive *in silico* skin permeation models.

Key Words: **skin sensitization; *in vitro*; skin permeation; *in silico*; mathematical modeling; area under the curve.**

The development of chemical-induced skin sensitization leading to allergic contact dermatitis represents a key consumer and occupational safety endpoint. Currently, animal tests, such as the local lymph node assay (LLNA, OECD, 2002), are often used to provide hazard characterization for risk assessments. However, there is interest in developing nonanimal approaches because of scientific advancements, ethical considerations, and upcoming legislation (EU, 2003; Fentem *et al.* 2004; Maxwell *et al.* 2008). It has been proposed that the integration of data from independent sources, each focused on one of the mechanistic steps required for induction of skin sensitization, could be used as a scheme to enable accurate hazard characterization using *in vitro* and *in silico* methods (Jowsey *et al.* 2006). Specifically, information about epidermal disposition, protein reactivity, epidermal inflammation, dendritic cell maturation, and T cell proliferation would cover the critical steps leading to induction. There is a growing body of work providing data on protein reactivity (Aleksic *et al.* 2009; Gerberick *et al.* 2007; Schultz *et al.* 2009), but established methods and data generation for the other steps are less developed at this stage. For example, an integrated approach has been described (Natsch *et al.* 2009), which closely follows the conceptual model of Jowsey *et al.* (2006), in which the majority of the data considered were measures of reactivity, both purely chemical and *in vitro* cell based, whereas epidermal disposition was simply represented by the octanol-water partition coefficient, log *P*. The aim of this work is to provide candidate parameters that describe epidermal disposition, together with the experimental and data analysis methods used to determine them, following the recommendations during European Centre for the Validation of Alternative Methods (ECVAM) workshop 59 for parameters that relate to the internal dose within the human epidermis under toxicologically relevant conditions (Basketter *et al.* 2007).

The measurements of epidermal disposition described here were obtained using the time course skin permeation experimental method developed by Pendlington *et al.* (2008). Standard *in vitro* flow-through diffusion cell experiments (OECD, 2004a,b) include measurement of the concentration in the skin only at the terminal sampling point to contribute to an estimate of systemic exposure over the duration of the experiment, whereas the time course method allows the kinetics of epidermal disposition to be determined. Pendlington *et al.* (2008) demonstrated the use of the method for the skin sensitizer cinnamic aldehyde applied in four different vehicles. In this work, data generated using the time course method are reported for a further 12 chemicals (10 sensitizers of various

degrees of potency and 2 nonsensitizers; benzaldehyde and 6-methylcoumarin) applied in acetone:olive oil (4:1, vol:vol, AOO), the preferred vehicle for the LLNA given by the OECD test guideline (OECD, 2002). Multicompartmental modeling has been used to determine the pharmacokinetic/toxicokinetic parameters that summarize the disposition kinetics, as suggested by Basketter *et al.* (2007): the maximum concentration (C_{max}) and the area under the curve (AUC) of concentration versus time. Basketter *et al.* (2007) proposed the use of the AUC at 120 h corresponding to the dose regimen of the LLNA. It is not clear what timescale for the AUC will be most relevant for integration with other sources of data to estimate hazard potency; consequently, we report both the AUC at 24 h (to correspond to the effect from a daily dose within that time frame) and at 120 h (to provide an estimation of the longer term retention of chemical in the skin following a single dose). It is hoped that consideration of both metrics, when combined with other sources of information, will indicate whether a shorter or longer timescale is more appropriate. Furthermore, although epidermal disposition is of primary interest because of the involvement of epidermal Langerhans' cells in skin sensitization induction (Griffiths *et al.*, 2005), we also report dermal disposition values because of the possible contribution from dermal dendritic cells (Fukunaga *et al.*, 2008; Kimber *et al.*, 2009).

The time course data presented here comprise a substantial and consistent set of detailed measurements of skin permeation kinetics, which could be a useful resource for the development of predictive spatial diffusion models of skin permeation, e.g., those by Chen *et al.* (2008) and Kasting *et al.* (2008). Such models provide *in silico* tools that could also contribute to an integrated approach to hazard characterization without new animal data. The experimental data reported in this work are therefore included as Supplementary data for the benefit of researchers with an interest in the field of skin permeation modeling.

MATERIALS AND METHODS

Chemicals. [^{14}C(U)]-hydroquinone and [ring-U-^{14}C]benzaldehyde were supplied by American Radiolabeled Chemicals Inc., St Louis, MO. α-Hexyl[U-^{14}C]cinnamic aldehyde, [ring-U-^{14}C]cinnamyl alcohol, 4-ethyl [U-^{14}C]resorcinol, [benzoyl-ring-U-^{14}C]phenyl benzoate, [2-^{14}C]dihydrocoumarin, [1-^{14}C]1-bromohexadecane, [1-^{14}C]bromododecane, [ring-U-^{14}C]-2,4-dinitrochlorobenzene, [coumarin-2-^{14}C]-6-methylcoumarin, and 3-methyl-4-[Ph-U-^{14}C]phenyl-[1,2,5]thiadiazole-1,1-dioxide were supplied by Selcia, Ongar, Essex, U.K.

1-Bromododecane was supplied by Alfa Aesar, Heysham, Lancashire, U.K. 3-Methyl-4-phenyl-1,2,5-thiadiazole-1,1-dioxide (MPT) was supplied by Tocris, Avonmouth, Bristol, U.K. 1,4-Dihydroquinone, α-hexylcinnamic aldehyde, benzaldehyde, cinnamic alcohol, 6-methylcoumarin, 4-ethylresorcinol, phenylbenzoate, 1-bromohexadecane, 3,4-dihydro-coumarin, 2,4-dinitrochlorobenzene, olive oil (highly refined, low acidity), PBS, newborn calf serum, penicillin-streptomycin solution, and amphotericin B were supplied by Sigma-Aldrich Company Limited, Gillingham, Kent, U.K. Aquasafe 500 liquid scintillation fluid was obtained from Zinsser Analytic, Maidenhead, Berkshire, U.K. Solvable, Soluene-250, HionicFluor liquid scintillation cocktail, and StarScint liquid scintillation cocktail were supplied by PerkinElmer LAS (U.K.) Limited, Beaconsfield, Buckinghamshire, U.K.

Skin samples. The skin samples were obtained from NHS Lothian, Livingston, U.K., or TCS CellWorks (who are supplied by BioPredic, France). Full-thickness human skin (from the abdomen or breast) was obtained from female patients who gave informed consent for their skin to be taken for scientific purposes prior to undergoing routine surgery. The skin was either processed by the procurer or processed in-house. For the latter, the skin was cleaned of subcutaneous fat and connective tissue using a scalpel blade. The skin samples were then wrapped in aluminum foil, placed in sealed plastic bags, and stored at approximately −20°C until used in the study. Human split-thickness skin (approximately 400 μm) was prepared from thawed skin samples using a Zimmer electric dermatome.

Experimental method. The skin samples were mounted in flow-through diffusion cells (Scott/Dick, University of Newcastle upon Tyne, U.K., or Crown Glass, Somerville, NJ), which were set in a heated steel manifold to give a skin surface temperature of 32°C. Receptor solution (PBS containing newborn calf serum [5%, wt/vol], amphotericin B [250 μg/ml], streptomycin [0.1 mg/ml], and penicillin G [100 units/ml]) was pumped through the cells for a 15-min equilibration period before dosing. This receptor solution was chosen because it is "physiologically conducive" (OECD, 2004b), and the solubility of each test item in this solution indicated that infinite sink conditions would be maintained throughout the experiment.

The test preparations were prepared in AOO (4:1, vol:vol) containing ethanol (5%, vol/vol) to aid solubility of the more lipophilic chemicals. In the case of MPT, post-dose stability testing indicated that the MPT was not stable in this vehicle; hence, the experiment was repeated with the vehicle AOO (4:1, vol:vol) containing tetrahydrofuran (5%, vol/vol) in which the MPT was shown to be stable. The concentration of test item in each test preparation is noted in Table 3 (see "Results" section). All chemicals were tested at a concentration of approximately 189mM, equal to the target molar concentration of cinnamic aldehyde in Pendlington *et al.* (2008). In addition, most chemicals were tested at a second concentration (e.g., approximately double or half 189mM) to investigate if the disposition kinetics varied with applied concentration.

A finite dose (25 μl/cm^2) was applied evenly over the stratum corneum surface of the exposed skin (surface area 0.64 or 0.38 cm^2). The donor chambers of the cells were occluded with an activated charcoal filter trap and cap to collect the volatile fraction. After dosing, receptor fluid was collected in hourly fractions from each cell. At each terminal time point (0.5, 1, 2, 4, 8, and 24 h), three or four cells were taken for mass balance calculations.

At each terminal time point, the carbon traps were removed from the cell and extracted with methanol. An aliquot (50 μl) of concentrated commercial soap was applied to the exposed skin and cleansed with tissue paper in a gentle rubbing motion, except in the case of α-hexylcinnamic aldehyde, 6-methylcoumarin, and MPT where this step was omitted because of the size of the aperture of the donor chambers of the Crown Glass diffusion cells (0.38 cm^2) being too small for this step to be performed. The skin was then rinsed with ten 0.5 ml aliquots of commercial hand wash soap solution diluted with water (soap, 2%, vol/vol); the washing process was then repeated. The skin was then removed from the cells and chemical extracted from the cells with methanol. Layers of stratum corneum were removed from the skin using D-Squame tape stripping discs; 10 discs were used for each skin sample, and each disc was analyzed individually. The tape-stripped skin was separated into exposed and flange (unexposed) areas and the epidermis of the exposed area was separated from the dermis by heat treatment. The exposed area of skin was wrapped in cling film and a 200-g brass weight, heated to 60°C, was applied for 90 s to the upper surface of the skin. The skin was then unwrapped and the epidermis removed by scraping with forceps. Tape strips and each skin subfraction were solubilized in Solvable or Soluene-350.

Radioactivity was determined by scintillation counting of each receptor solution fraction, skin rinse, skin swab, cell rinse, tape strip, epidermis, dermis, flange skin, and carbon trap.

Octanol-water partition coefficients. Where available, experimental values from the SRC PhysProp database (http://www.srcinc.com) have been used; otherwise, the log P was predicted from molecular structure using BioByte ClogP 4.0. The values are listed in Table 3.

Overview of modeling methods. Multicompartmental models were used to estimate toxicokinetic parameters from the time course data. The models were similar in compartmental structure to those reviewed by McCarley and Bunge (2001), with the exception that those discussed in the review were predictive models with parameters derived from physicochemical properties of the permeating chemical, whereas the parameters of models applied in this work were determined by optimizing the fit of the model to the data. We considered four different compartmental models in a selection process before further investigation of the data using the preferred model. The following section describes features common to all four models.

The sets of data samples identified as being associated with each compartment and abbreviations used for them are listed in Table 1.

Flows of chemical between compartments are governed by the dominant physical processes involved in skin permeation, which are Fickian diffusion driven by concentration gradients and partitioning according to hydrophobicity (Nitsche and Kasting, 2008). Other possible effects such as reversible or irreversible binding to skin proteins or metabolic conversion are not included in the models. In general, the rate of change of amount of chemical (m_j, in moles) in compartment j, which has adjacent compartments i and k, is given by Equation 1 below, equivalent to Equations 4–6 described by McCarley and Bunge (2001).

$$\dot{m}_j = \left(k_{ij}c_i - k_{ji}c_j\right) - \left(k_{jk}c_j - k_{kj}c_k\right). \tag{1}$$

This equation describes transport of the test chemical between compartments, as given by diffusion flows proportional to concentrations (e.g., c_j, in moles per cubic centimeter). The ratio of the permeation coefficients k_{ji} to k_{ij} is equivalent to the partition coefficient between adjacent compartments or steady-state c_i/c_j ratio. First-order loss terms were included for evaporation from the donor phase and for transport from the final skin compartment to the receptor fluid (an infinite sink). Many of the chemicals tested here were volatile, and in those cases, the mass balance was observed to decrease over time. The models included no mechanism for overall loss from the system apart from evaporation. The total thickness of the skin compartments was set at 400 μm, which was the level to which the skin membranes were dermatomed before being mounted in the diffusion cells. The total thickness of the stratum corneum was assumed to be 10 μm and the thickness of the epidermis 90 μm, both of which are values consistent with those typically used for these layers (McCarley and Bunge 2001; Nitsche and Kasting, 2008). Fitting of model parameters was performed using nonlinear optimization to search for the parameter set that gave the minimum residual sum of squared errors (RSS) between the model and the data (using the lsqnonlin algorithm in MATLAB). In each case, 100 optimizations starting from randomized initial values were performed in order to avoid local minima as far as possible. The C_{max} parameter in the epidermis is the maximum value of the concentration in that compartment as a function of time:

$$C^{E}_{max} = \max_t\left[c_E(t)\right]. \tag{2}$$

The AUC up to any time T in the epidermis is calculated by integration of the concentration:

$$\mathrm{AUC}^{E}_{T} = \int_0^T c_E(t)\mathrm{d}t. \tag{3}$$

The C_{max} and AUC in the dermis are obtained similarly from the concentration in that compartment.

Model with one skin compartment. The one-skin compartment model, the simplest considered, was analogous in structure to the one-compartment models reviewed by McCarley and Bunge (2001) or model 3 described by Saiyasombati and Kasting (2003). As shown schematically in Figure 1, the layers of skin were represented by a single compartment (S for skin). The kinetic behavior for the one-skin compartment model was as described by Equation 4:

$$\begin{aligned}\dot{m}_{DP} &= -e_{DP}c_{DP} - k_{DP:S}c_{DP} + k_{S:DP}c_S,\\ \dot{m}_S &= k_{DP:S}c_{DP} - k_{S:DP}c_S - e_Sc_S,\\ \dot{m}_{RF} &= e_Sc_S.\end{aligned} \tag{4}$$

TABLE 1
Definitions of Compartments in Terms of the Associated Data Samples

Samples	Compartment	Time points sampled
The tissue swabs, skin wash, and cell wash, which combined to give the amount of test chemical remaining on the skin surface	Donor phase (DP)	30 min and 1, 2, 4, 8, and 24 h
The 10 tape strips	Stratum corneum (SC)	30 min and 1, 2, 4, 8, and 24 h
The portion of skin removed after heat treatment plus the cling film (plastic wrap) used in that process	Epidermis (E)	30 min and 1, 2, 4, 8, and 24 h
The remaining skin after heat treatment	Dermis (D)	30 min and 1, 2, 4, 8, and 24 h
All collected receptor fluid samples	Receptor fluid (RF)	30 min and every hour from 1 to 24 h

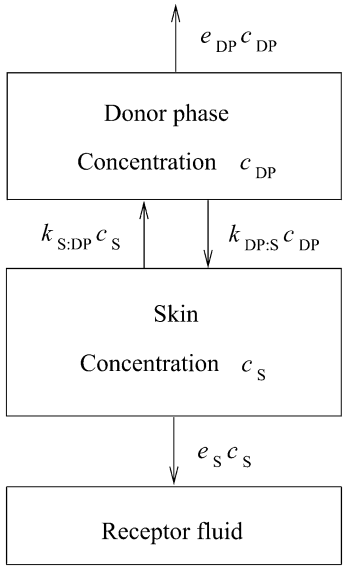

FIG. 1. Structure of one-skin compartment model.

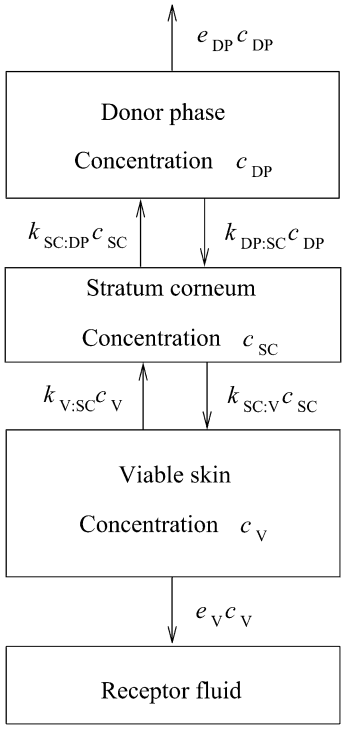

FIG. 2. Structure of two-skin compartment model.

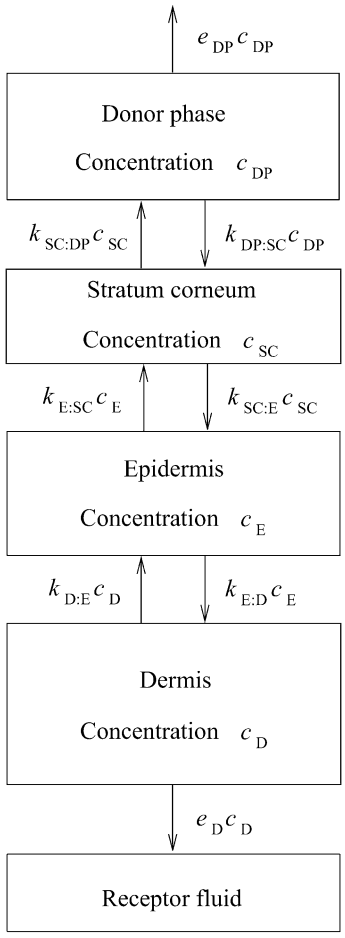

FIG. 3. Structure of three-skin compartment model.

The parameters e_{DP} and e_S were the proportionality constants for evaporative loss from the donor phase and flow of chemical from the skin to the receptor fluid, respectively. The data for the amount of chemical in the skin compartment were derived by summing the amounts in the stratum corneum, epidermis, and dermis at each time point. In order to predict the amount of chemical in an individual skin layer as a function of time t, e.g., m_E (t) in the epidermis, the amount in the skin compartment from the model, m_S (t), was multiplied by a time-independent fraction, φ_E. The value of the φ_E fraction was estimated as the sum of all data points over the time course for the epidermis layer divided by the same sum for all skin layers (stratum corneum plus epidermis plus dermis). Generally, if j = SC, E, or D and $M_{j,\alpha}$ is the measured amount of chemical in layer j at time point α (0.5, 1, 2, 4, 8, or 24 h), then:

$$\begin{aligned} m_j(t) &= \varphi_j m_s(t), \\ \varphi_j &= \frac{\sum_{\alpha} M_{j,\alpha}}{\sum_{\alpha}\left(M_{SC,\alpha}+M_{E,\alpha}+M_{D,\alpha}\right)}, \\ \varphi_{SC} &+ \varphi_E + \varphi_D = 1. \end{aligned} \tag{5}$$

The one-skin compartment model had six parameters: $k_{DP:S}$, $k_{S:DP}$, e_{DP}, e_S, and two independent φ ratios.

Model with two skin compartments. The two-skin compartment model was similar to the two-compartment models discussed by McCarley and Bunge (2001) and had a separate stratum corneum compartment plus a viable skin (V) compartment (see Fig. 2 and Equation 6). The data for the amount of chemical in the viable skin compartment were derived by summing the amounts in the epidermis and dermis at each time point. The two-skin compartment model had seven parameters, including one independent ψ ratio to allow predictions for the epidermis and dermis layers from viable skin compartment values, in a similar way to that described for the previous model.

$$\begin{aligned} \dot{m}_{DP} &= -e_{DP}c_{DP} - k_{DP:SC}c_{DP} + k_{SC:DP}c_{SC}, \\ \dot{m}_{SC} &= k_{DP:SC}c_{DP} - k_{SC:DP}c_{SC} - k_{SC:V}c_{SC} + k_{V:SC}c_{V}, \\ \dot{m}_{V} &= k_{SC:V}c_{SC} - k_{V:SC}c_{V} - e_{V}c_{V}, \\ \dot{m}_{RF} &= e_{V}c_{V}, \\ m_j(t) &= \psi_j m_v(t);\ \ j = E, D, \\ \psi_j &= \frac{\sum_{\alpha} M_{j,\alpha}}{\sum_{\alpha}\left(M_{E,\alpha}+M_{D,\alpha}\right)}, \\ \psi_E &+ \psi_D = 1. \end{aligned} \tag{6}$$

Model with three skin compartments. The three-skin compartment model had individual compartments for stratum corneum, epidermis, and dermis layers and eight parameters (see Fig. 3 and Equation 7).

$$\begin{aligned} \dot{m}_{DP} &= -e_{DP}c_{DP} - k_{DP:SC}c_{DP} + k_{SC:DP}c_{SC}, \\ \dot{m}_{SC} &= k_{DP:SC}c_{DP} - k_{SC:DP}c_{SC} - k_{SC:E}c_{SC} + k_{E:SC}c_{E}, \\ \dot{m}_{E} &= k_{SC:E}c_{SC} - k_{E:SC}c_{E} - k_{E:D}c_{E} + k_{D:E}c_{D}, \\ \dot{m}_{D} &= k_{E:D}c_{E} - k_{D:E}c_{D} - e_{D}c_{D}, \\ \dot{m}_{RF} &= e_{D}c_{D}. \end{aligned} \tag{7}$$

Finite difference model. The finite difference model was similar to the three-skin compartment model, except that the donor phase and all skin layers were each divided into 10 equal volume compartments. This made it a finite difference version of the continuous membrane models advocated by McCarley

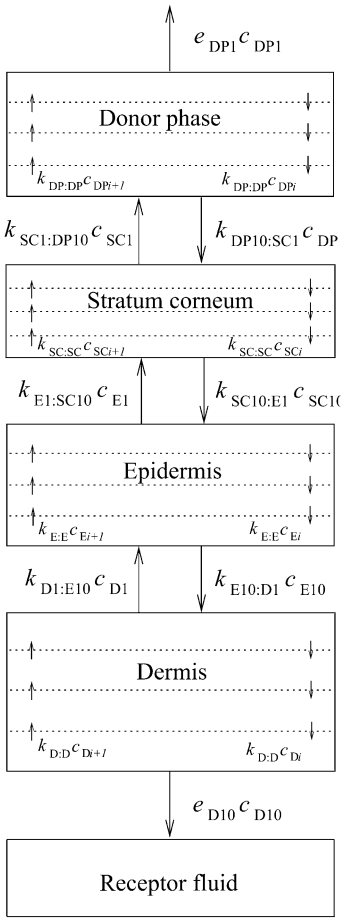

FIG. 4. Structure of finite difference model. In the analysis, there were 10 compartments per skin layer (plus donor phase); however, only four are illustrated for simplicity.

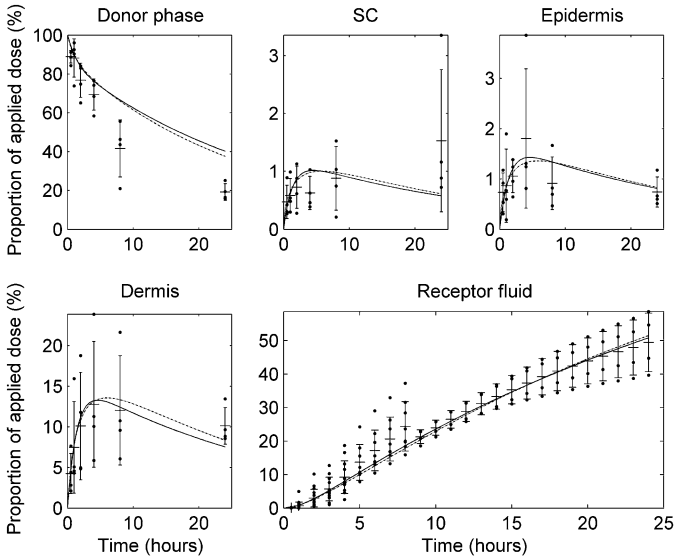

FIG. 5. Fits of two-skin compartment model (solid line) and finite difference model (dashed line) to mean data across all donors (plus signs, +) for cinnamic alcohol at 192mM in AOO. Points: single measurements from each donor/diffusion cell. Error bars: SD of data across all donors/diffusion cells sampled at each time point.

and Bunge (2001); both types allow the description of concentration gradients across skin layers and time lags because of diffusion across a layer, where a lower resolution compartmental approach assumes uniform concentration throughout each compartment and no time delay to achieve this equilibration. The equations of the finite difference model were derived in the same way as those of the models described above and are not presented because the level of detail would not make them instructive. Uniform properties were assumed within each layer, so, e.g., in the epidermis if a, b, and c label compartments between 1 and 10, then $k_{Ea:Eb} = k_{Eb:Ec}$ (homogeneity) and $k_{Ea:Eb} = k_{Eb:Ea}$ (intralayer partition coefficients equal to unity). Partitioning from one layer to another was included (e.g., between the epidermis and dermis, $k_{E10:D1}$ was not set equal to $k_{D1:E10}$). With these assumptions, the finite difference model had 12 parameters, as indicated in Figure 4. The C_{max} and AUC were calculated after summing the amount of chemical in the 10 compartments to obtain a total amount in that layer.

Model selection. Each data set consists of results for the donor phase, skin layers, and receptor fluid for three or four skin donors and several time points. Averaging the results across donors gives a single time course for each compartment, and the four models described above were fitted to this mean time course for each data set in order to compare models and select a preferred one. Figure 5 gives an example of a complete data set, together with fits of the two-skin compartment model and finite difference model to the mean data across donors. The models were compared according to the RSS between each model's predictions and the data and also using the Bayesian information criterion (BIC; Kass and Raftery, 1995; Schwarz, 1978) for p parameters and n data points:

$$\mathrm{BIC} = n\log_e \mathrm{RSS} + p\log_e n \quad (8)$$

As Equation 8 shows, the BIC is a combined measure of model accuracy (given by the first term on the right hand side, involving RSS) and model complexity (the second term, proportional to the number of parameters of the model). Selection of models by choosing the lowest BIC instead of the lowest RSS acts against overfitting or inclusion of unnecessary parameters. Absolute values of BIC are not meaningful; it is only the differences between the BIC for different models calculated with the same data set that are useful. For each data set, the four BIC values obtained for the four models under consideration were shifted together so that the lowest BIC was set equal to zero.

Uncertainty and variability of epidermal disposition parameters. The preferred model from the selection process was also fitted to the time courses associated with each individual skin donor; Figure 6 shows an example of a fit to the mean data across skin donors and a fit to data for a single donor for the same chemical. Fitting to individual donor time courses gave three or four values of C_{max} and AUC for each data set, which provided information about the uncertainty of these parameters. This was not purely from donor variation, as there was one cell per skin donor per time point, and some variation would be expected from one diffusion cell to another even with the same donor (Chilcott *et al.*, 2005). Therefore, the variation found was because of a combination of donor and cell variability.

Investigation of possible reduced time course protocol. The preferred model was fitted to time courses based on the mean data across skin donors but with a reduced number of time points for the donor phase and skin layers. This helped assess the feasibility of a reduced time course skin permeation experiment with results (disposition kinetics parameters AUC and C_{max}) that approximate those derived from full time course data. All time courses included the hourly collection of receptor fluid from the diffusion cells sampled at the 24-h terminal time point. For the donor phase and skin layer results, the following were investigated: data from cells sampled at 0.5 and 24 h, 1 and 24 h, 2 and 24 h, 4 and 24 h, 8 and 24 h, and finally data from the cells sampled at

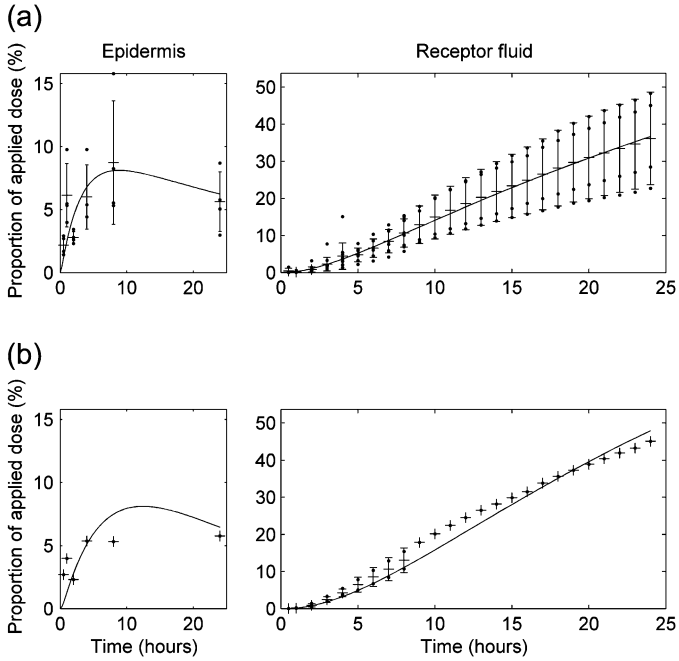

FIG. 6. Fits of two-skin compartment model (solid lines) to (a) mean data across all donors (plus signs, +) and to (b) data from one skin donor (plus signs, +) for 1,4-dihydroquinone at 76mM in AOO. Points: single measurements from each donor/diffusion cell. Error bars: SD of data across all donors/diffusion cells sampled at each time point.

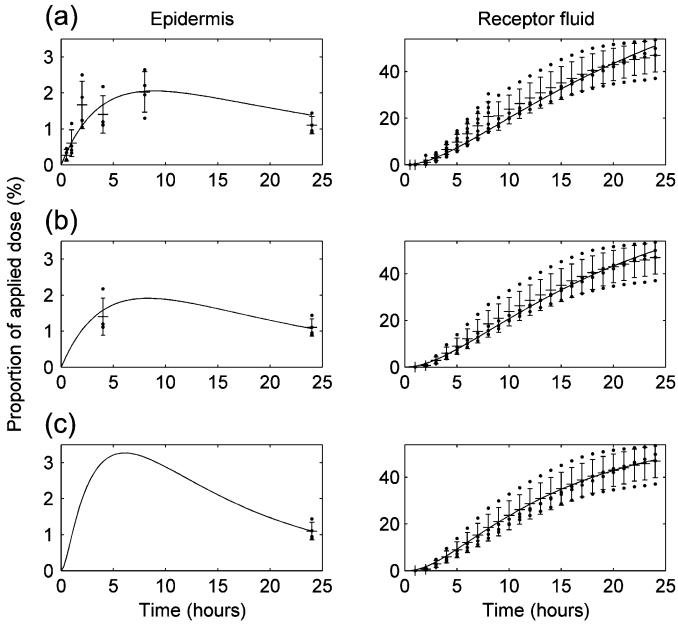

FIG. 7. Fits of two-skin compartment model (solid lines) to mean data across all donors (plus signs, +) for cinnamic aldehyde at 187mM in propylene glycol (PG) using data from (a) the full time course, (b) a reduced time course with donor phase and skin layer data from diffusion cells sampled and 4 and 24 h, and (c) a reduced time course from cells sampled at the final time point of 24 h only. Points: single measurements from each donor/diffusion cell. Error bars: SD of data across all donors/diffusion cells sampled at each time point.

24 h only. This last data set corresponds to the data available from a standard *in vitro* skin permeation assay, including only a single time point rather than a time course for the donor phase and skin layers; nevertheless, model fitting was possible because of the kinetic information available from the receptor fluid data. Figure 7 shows example fits of the selected two-skin compartment model to full time course data, a reduced time course with donor phase and skin layer data from diffusion cells sampled and 4 and 24 h, and a reduced time course from cells sampled at the final time point of 24 h only.

For the reduced time course that provided the closest approximation to the full time course disposition kinetics parameters, model fits to the individual skin donor time courses were produced in order to allow comparison of the reduced and full time course disposition kinetics parameters including uncertainty in both cases.

RESULTS

Model Selection

The finite difference model fitted with the lowest RSS error for 18 out of 26 data sets. It would generally be expected that the most complex models give the lowest error. The reason this has not occurred for eight data sets is that in those cases, the error of one or more of the simpler compartmental models is very close to that of the finite difference model (within 1.2% or less), and there is then some chance that the compartmental model error will be smaller because of the randomization of initial values. From 26 data sets, 11 had the lowest BIC with the one-skin compartment model, 12 with the two-skin compartment model, and the remaining three with the three-skin compartment model. On this basis, the two-skin compartment model was selected as the preferred model giving the best compromise of accuracy without unnecessary complexity for the greatest number of data sets. Table 2 lists the RSS and BIC for all four models and each data set, with the lowest RSS and BIC values highlighted.

Epidermal Disposition Parameters Including Uncertainty

Table 3 details the chemicals under investigation, the vehicles used, the concentrations of the chemicals as applied in the test preparation (C_{applied}), whether there were three or four skin donors (and diffusion cells for each time point), and the log P of the chemicals. Table 3 also lists the overall results for the data sets analyzed in this work: the AUC_{120}, AUC_{24}, and $C_{\max}$ parameters for the epidermis and dermis calculated using the selected two-skin compartment model for all data sets by fitting to the data for individual donors to give estimates of uncertainty of the disposition kinetics parameters.

Figure 8 demonstrates the comparison between the AUC_{24} in the epidermis calculated by fitting to individual donor time courses and the same parameter from fitting the two-skin compartment model to the mean data across all donors (obtained as part of the model selection process).

TABLE 2
RSS and BIC Values from All Four Models Investigated for Each Data Set

	RSS				BIC			
Data set identification number	1	2	3	FD	1	2	3	FD
1	3.08	2.56	2.52	**2.15***	5.02	**0.00***	3.09	10.82
2	2.06	**1.90***	1.91	1.92	**0.00***	0.08	4.07	19.90
3	1.93	1.66	1.67	**1.56***	3.44	**0.00***	4.16	16.35
4	3.08	3.02	3.02	**2.72***	**0.00***	2.88	6.89	17.19
5	7.26	7.14	7.09	**5.59***	**0.00***	3.09	6.60	10.52
6	6.40	6.36	6.33	**5.03***	**0.00***	3.58	7.30	11.59
7	3.97	**3.01***	3.01	3.01	9.67	**0.00***	3.90	19.51
8	4.64	2.58	2.58	**2.55***	24.87	**0.00***	3.87	18.96
9	1.25	0.97	0.97	**0.87***	8.46	**0.00***	3.85	13.93
10	2.83	**2.50***	2.51	2.51	2.16	**0.00***	3.95	19.48
11	**2.80***	2.82	2.84	2.81	**0.00***	4.39	8.51	23.58
12	1.25	1.04	1.00	**0.96***	4.89	**0.00***	2.01	15.42
13	2.00	1.84	1.85	**1.82***	0.02	**0.00***	3.92	18.72
14	1.45	1.45	1.37	**1.24***	**0.00***	4.11	5.24	15.88
15	3.43	2.71	**2.70***	2.72	7.59	**0.00***	3.71	19.55
16	2.63	2.59	2.56	**2.45***	**0.00***	3.22	6.43	19.91
17	6.84	6.72	**6.41***	6.49	**0.00***	3.04	4.61	20.75
18	2.21	2.13	1.96	**1.72***	**0.00***	2.02	1.96	11.13
19	1.71	1.29	1.28	**1.23***	10.02	**0.00***	3.52	17.38
20	4.93	3.73	2.64	**2.62***	22.83	13.17	**0.00***	15.21
21	1.00	0.98	0.55	**0.51***	21.17	24.23	**0.00***	12.08
22	4.63	1.14	1.14	**0.95***	64.97	**0.00***	4.03	10.57
23	3.53	3.15	**2.96***	2.96	1.71	**0.00***	0.90	16.50
24	11.47	8.60	**6.67***	6.69	18.80	8.59	**0.00***	15.70
25	5.33	5.34	5.13	**4.96***	**0.00***	4.00	5.89	19.84
26	5.36	5.12	4.72	**4.53***	**0.00***	1.57	1.54	15.03

Note. Model labels: 1, 2, and 3 refer to one-, two-, and three-skin compartment models, respectively; FD is finite difference model. Asterisks and bold type show the lowest RSS or BIC for each data set. See Table 3 for details of each data set according to its identification number.

Investigation of Possible Reduced Time Course Protocol

In order to determine what would be an optimal reduced time course protocol, the relative errors were calculated between the disposition kinetics parameters obtained from each reduced time course and those from the full time course data. The sums of the squared relative errors over all data sets for each disposition kinetics parameter are plotted in Figure 9. It is clear from this chart that the reduced time course with time points at 4 and 24 h provides the closest agreement with the disposition kinetics parameters from full time course data. As an example, Figure 10 shows the concordance between the epidermal AUC_{24} derived from a reduced time course of 4- and 24-h time points and the same parameter from the full time course data for all 26 data sets, including error bars on all estimates from fitting to individual skin donor data.

Lack of Correlation between Disposition Kinetics Parameters and Log P

Table 4 lists the Spearman rank correlation coefficients between the AUC and C_{max} parameters and log *P* based on the results presented in Table 3.

DISCUSSION

In this work, we have provided candidate information on epidermal disposition to be integrated with other novel nonanimal data sources for skin sensitization hazard characterization via the generation of new time course skin permeation data. We have summarized the data in the form of toxicokinetic parameters, AUC and C_{max} in the epidermis and dermis, through the use of a multicompartmental model. The model selected as the best compromise between accuracy and complexity had a separate compartment for the stratum corneum but a combined compartment for the epidermis and dermis. Similar models have been used by other researchers, and this structure is intuitively reasonable given the differing properties of the stratum corneum and the epidermis or dermis for diffusion and partitioning of permeant chemicals, especially the high lipid content of the stratum corneum.

It is well known that log *P* has a dominant effect on steady-state flux of chemicals through skin (Potts and Guy, 1992), and it has been used as a proxy parameter for epidermal disposition when integrating different sources of information (Natsch *et al*., 2009; Roberts *et al*., 2008). However, the transient, finite

TABLE 3

Estimates of the Disposition Kinetics Parameters (AUC and C_{max}) in the Epidermis and Dermis, for All Data Sets, Derived from Fits of the Two-Skin Compartment Model to the Time Course Data for Individual Skin Donors to Provide Information on the Uncertainty of the Parameters

							$AUC^{E}_{120}/C_{applied}$ (h)			$AUC^{E}_{24}/C_{applied}$ (h)			$C^{E}_{max}/C_{applied}$ (dimensionless)			$AUC^{D}_{120}/C_{applied}$ (h)			$AUC^{D}_{24}/C_{applied}$ (h)			$C^{D}_{max}/C_{applied}$ (dimensionless)		
Data set identification number	Supplementary data file number[a]	Test chemical	Vehicle	Measured concentration, $C_{applied}$ (mM)	Number of donors	Log *P*	Average	Lower limit of range	Upper limit of range	Average	Lower limit of range	Upper limit of range	Average	Lower limit of range	Upper limit of range	Average	Lower limit of range	Upper limit of range	Average	Lower limit of range	Upper limit of range	Average	Lower limit of range	Upper limit of range
1	26	1,4-Dihydroquinone	AOO	76	4	0.59[b]	11	9	14	4.4	3.0	6.6	0.22	0.14	0.34	4.6	3.7	5.8	1.9	1.5	2.3	0.091	0.073	0.115
2	27	1,4-Dihydroquinone	AOO	191	4	0.59[b]	5.2	2.4	11.0	2.3	1.6	3.4	0.13	0.10	0.15	3.6	2.1	6.2	1.6	1.2	2.2	0.088	0.067	0.117
3	33	MPT	AOO	205	3	1.44[c]	18	12	27	5.4	4.2	7.1	0.25	0.20	0.32	1.5	0.8	2.8	0.47	0.31	0.71	0.022	0.015	0.032
4	34	MPT	AOOthf	146	3	1.44[c]	9.8	5.3	18.2	2.5	1.5	4.0	0.11	0.07	0.17	0.65	0.35	1.22	0.17	0.10	0.26	0.0073	0.0048	0.0112
5	12	Benzaldehyde	AOO	191	4	1.48[b]	0.18	0.09	0.37	0.16	0.09	0.28	0.018	0.011	0.028	0.12	0.07	0.22	0.11	0.07	0.18	0.012	0.007	0.022
6	13	Benzaldehyde	AOO	2359	4	1.48[b]	0.57	0.42	0.78	0.38	0.28	0.52	0.022	0.016	0.029	0.34	0.30	0.39	0.23	0.19	0.27	0.013	0.010	0.016
7	24	3,4-Dihydrocoumarin	AOO	191	4	1.63[c]	0.95	0.68	1.32	0.49	0.31	0.79	0.026	0.015	0.043	1.8	1.2	2.7	0.92	0.72	1.18	0.048	0.038	0.060
8	25	3,4-Dihydrocoumarin	AOO	380	4	1.63[c]	1.4	1.1	1.8	0.55	0.41	0.75	0.028	0.020	0.038	3.1	2.4	3.9	1.2	0.9	1.7	0.062	0.045	0.085
9	30	4-Ethylresorcinol	AOO	191	4	1.84[c]	2.3	2.0	2.7	1.3	1.0	1.8	0.074	0.054	0.103	3.8	3.2	4.4	2.1	1.6	2.8	0.12	0.09	0.16
10	31	4-Ethylresorcinol	AOO	399	4	1.84[c]	1.8	1.4	2.4	1.2	1.0	1.6	0.080	0.057	0.111	4.4	2.6	7.2	3.0	2.2	4.0	0.19	0.17	0.22
11	23	Cinnamic aldehyde[d]	PG	182	4	1.9[b]	2.0	1.6	2.4	1.1	1.0	1.2	0.058	0.049	0.067	2.0	1.5	2.5	1.1	1.0	1.2	0.057	0.049	0.067
12	21	Cinnamic aldehyde[d]	AqEtOH	185	4	1.9[b]	1.3	0.9	1.9	1.4	1.0	1.9	0.26	0.23	0.30	1.4	1.1	1.7	1.4	1.2	1.8	0.27	0.26	0.29
13	22	Cinnamic aldehyde[d]	EtOH	187	4	1.9[b]	1.6	1.0	2.6	1.6	1.0	2.4	0.18	0.12	0.26	1.8	1.1	3.1	1.7	1.0	2.9	0.20	0.13	0.32
14	20	Cinnamic aldehyde[d]	AOO	195	4	1.9[b]	2.1	1.4	3.2	1.3	0.9	2.0	0.072	0.048	0.106	2.8	2.1	3.6	1.8	1.3	2.3	0.096	0.074	0.123
15	32	6-Methylcoumarin	AOO	203	3	1.91[c]	0.85	0.64	1.14	0.46	0.40	0.53	0.025	0.022	0.030	0.91	0.74	1.12	0.49	0.39	0.62	0.027	0.020	0.037
16	18	Cinnamic alcohol	AOO	192	4	1.95[b]	1.3	0.9	1.9	0.71	0.46	1.11	0.039	0.024	0.063	3.6	2.6	5.0	2.0	1.4	3.0	0.11	0.07	0.17
17	19	Cinnamic alcohol	AOO	1510	4	1.95[b]	1.4	1.3	1.6	0.38	0.28	0.53	0.021	0.017	0.026	5.1	3.5	7.6	1.4	1.2	1.6	0.073	0.059	0.092
18	28	DNCB	AOO	99	4	2.17[b]	5.9	4.6	7.5	1.2	0.9	1.6	0.068	0.056	0.081	3.9	3.2	4.7	0.80	0.68	0.93	0.045	0.035	0.058
19	29	DNCB	AOO	189	4	2.17[b]	3.2	2.4	4.2	0.79	0.55	1.16	0.039	0.026	0.057	2.2	2.0	2.4	0.54	0.39	0.75	0.027	0.018	0.038
20	36	Phenylbenzoate	AOO	187	4	3.59[b]	1.1	0.5	2.5	0.25	0.18	0.36	0.014	0.008	0.023	1.0	0.3	3.5	0.22	0.10	0.52	0.012	0.004	0.034
21	37	Phenylbenzoate	AOO	379	4	3.59[b]	0.54	0.19	1.53	0.19	0.12	0.31	0.010	0.007	0.015	0.58	0.20	1.69	0.21	0.12	0.35	0.011	0.007	0.018
22	35	αHCA	AOO	177	3	5[c]	3.5	1.4	8.9	0.50	0.32	0.78	0.032	0.017	0.058	0.35	0.17	0.70	0.049	0.040	0.061	0.0031	0.0021	0.0046
23	14	1-Bromododecane	AOO	189	4	6.9[c]	7.6	3.0	19.1	1.1	0.8	1.5	0.069	0.048	0.098	1.2	0.5	2.6	0.17	0.11	0.26	0.011	0.008	0.015
24	15	1-Bromododecane	AOO	723	4	6.9[c]	28	22	35	1.3	0.9	1.8	0.11	0.08	0.14	4.4	3.6	5.4	0.20	0.18	0.22	0.017	0.015	0.019
25	16	1-Bromohexadecane	AOO	189	4	9.01[c]	1.3	0.8	2.2	0.39	0.25	0.63	0.019	0.011	0.033	0.13	0.06	0.26	0.039	0.012	0.126	0.0018	0.0005	0.0068
26	17	1-Bromohexadecane	AOO	379	4	9.01[c]	1.6	0.4	6.2	0.29	0.16	0.51	0.017	0.009	0.034	0.20	0.04	1.05	0.037	0.015	0.093	0.0022	0.0007	0.0067

Note. The average is the geometric mean over results from individual donors, and the range of uncertainty is given by one geometric SD either side; i.e., the lower limit of the range is the geometric mean divided by the geometric SD and the upper limit is the geometric mean multiplied by the geometric SD. Values of AUC (in (millimoles per cubic centimeter) × hours) and C_{max} (in millimoles per cubic centimeter) have been normalized by the concentration of the chemical in the applied test preparation, $C_{applied}$ (in millimoles per cubic centimeter = Molar), to allow direct comparison between different concentrations. Therefore, the quoted values of $AUC/C_{applied}$ have units of hours and those of $C_{max}/C_{applied}$ are dimensionless. DNCB = 1-chloro-2,4-dinitrobenzene; αHCA, α-hexylcinnamic aldehyde; AOOthf, acetone:olive oil (4:1, vol:vol) containing 5% (vol:vol) tetrahydrofuran; PG, propylene glycol; aqEtOH, aqueous ethanol (1:1, vol:vol); EtOH, ethanol.

[a]The name of the Supplementary data file corresponding to each data set is in the form toxsci-10-0743-File0*nn*.xls with *nn* given by the numbers in this column.

[b]Experimental log Kow value obtained from SRC PhysProp database.

[c]Predicted log *P* value from BioByte ClogP 4.0.

[d]From data presented in Pendlington *et al.* (2008).

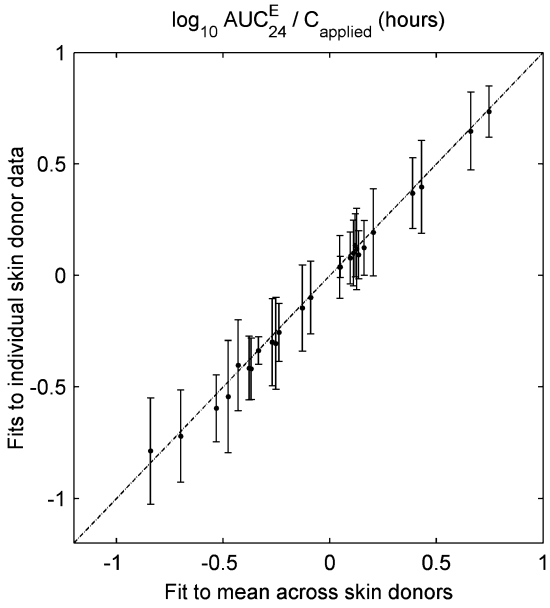

FIG. 8. Comparison of the AUC_{24} in the epidermis for all data sets calculated by fitting the two-skin compartment model to the mean data across all donors (horizontal axis) to that derived by fitting to individual donor time courses (vertical axis). For the latter, the center of each error bar is the geometric mean over results from individual donors, and the limits of the error bar show one geometric SD either side. Dashed line is 1:1 line.

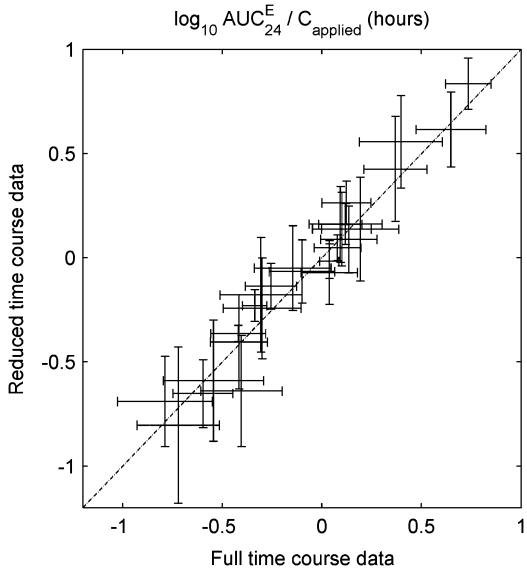

FIG. 10. Comparison of the AUC_{24} in the epidermis for all data sets calculated by fitting the two-skin compartment model to full time course data (horizontal axis) to that derived by fitting to the reduced time course of 4- and 24-h time points (vertical axis). In both cases, individual skin donor data have been used to estimate uncertainty; the center of each error bar is the geometric mean over results from individual donors, and the limits of the error bar show one geometric SD either side. Dashed line is 1:1 line.

dose concentration of chemical in the epidermis, as summarized by the AUC or C_{max}, does not correlate with log P, as shown by the results in Table 4. The disposition kinetics parameters therefore represent independent information, probably because they are derived from an experiment with a finite dose and nonaqueous vehicle, whereas log P is known to be an important factor in transport through skin for conditions of infinite dose in an aqueous vehicle. The AUC at 24 h and the C_{max} in the dermis may be weakly, negatively correlated to log P (the significance is just outside the 5% level); this effect is produced by low values of these disposition parameters for the most hydrophobic chemicals tested (those with log $P > 3$) because of their low rate of permeation through the dermis.

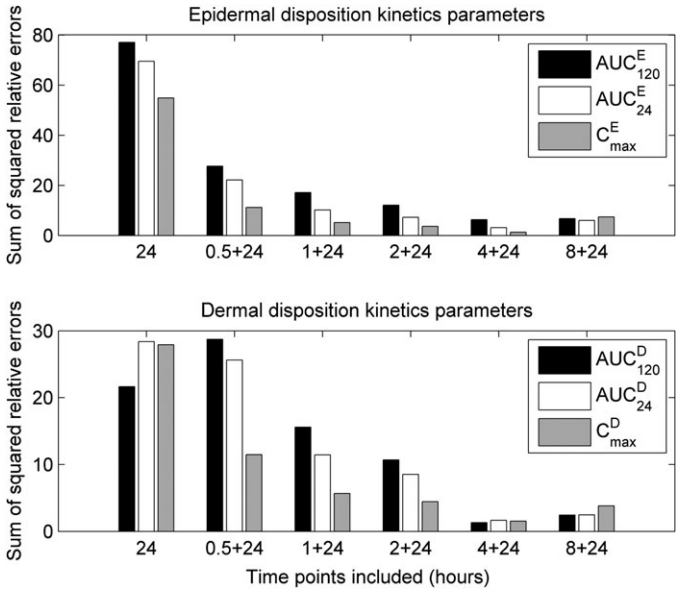

FIG. 9. The sum over all data sets of the squared relative error between the disposition kinetics parameters calculated using reduced time course data and those derived from the full time course available. Reduced time courses investigated were data from the cells sampled at 24 h only (labeled as ''24''; left hand side), data from cells sampled at 0.5 and 24 h (labeled as ''0.5 + 24''; similarly for others), 1 and 24 h, 2 and 24 h, 4 and 24 h, 8 and 24 h.

TABLE 4
Spearman rank correlation coefficients and *p* Values between Disposition Kinetics Parameters and Log *P*

Parameter	Spearman rank correlation coefficient	*p* Value
$AUC^{E}_{120}/C_{applied}$	−0.03	0.92
$AUC^{E}_{24}/C_{applied}$	−0.47	0.11
$C^{E}_{max}/C_{applied}$	−0.40	0.18
$AUC^{D}_{120}/C_{applied}$	−0.29	0.33
$AUC^{D}_{24}/C_{applied}$	−0.54	0.06
$C^{D}_{max}/C_{applied}$	−0.53	0.07

Note. For chemicals tested at two concentrations, the disposition kinetics parameters for the two concentrations were averaged to give a single value for each chemical. For cinnamic aldehyde and MPT, the disposition kinetics parameters with AOO vehicle were taken for consistency with the vehicle for other data sets.

There is also no correlation between the epidermal disposition kinetics parameters of the sensitizers investigated in this work and the LLNA effective concentration for 3-fold stimulation (EC_3) potency values of those chemicals. This is not surprising because the epidermal disposition kinetics parameters have been measured for human skin and the LLNA EC_3 provides an assessment of the sensitizing potency in mice. Also, epidermal disposition is not expected to be the most significant factor influencing the sensitization potency; e.g., in the framework of Jowsey *et al.* (2006), it was assigned a range of two possible scores compared with five for protein reactivity, dendritic cell maturation, and T cell proliferation. As shown in Figures 8 and 10, the epidermal disposition parameters found for different chemicals span about two orders of magnitude, and comparison with the size of the error bars, typically half an order of magnitude for two geometric SDs, indicates that at least three scores or classes of epidermal disposition could be motivated. However, for maximum use of information, parameters that take continuous values, e.g., epidermal disposition as described here, should be integrated as continuous parameters without reduction to a small number of possible scores.

The level of importance of epidermal disposition in an integrated approach to hazard characterization remains to be determined and to do so requires further data, for more chemicals, to be generated for this and other lines of evidence. Further generation of epidermal disposition kinetics data could include a greater number of nonsensitizers, of which the most interesting cases are similar to the two included here, benzaldehyde and 6-methylcoumarin, which have electrophilic reactive groups (Roberts *et al.*, 2007), and whose status as nonsensitizers therefore requires explanation.

We have demonstrated experimental and modeling methods for generation of epidermal disposition kinetics parameters for a small number of chemicals. Expanding this to a much greater number of chemicals is problematic because the time course skin permeation experiment is resource intensive and low throughput. Predictive *in silico* models of skin permeation, as discussed in the "Introduction" section, may be advantageous in this respect; however, the development of these models is also limited by availability of data. The reduced time course version of the experiment proposed in this work is one potential tool for generating time course skin permeation data at lower cost per chemical and higher throughput. If possible, when designing skin permeation experiments, the information requirements of predictive *in silico* models based on their state of development at the time should also be considered, in order to aid progress with models and subsequent efficiency of experiments, and improve understanding of skin permeation through a dialogue between experimental and computational approaches.

Future work to continue developing methods to determine epidermal disposition kinetics could include a comparison between the *in vitro* methods discussed in this work and time course *in vivo* measurements, in particular for sensitizing or electrophilic chemicals. Also, a standard vehicle (AOO) was used here for all chemicals wherever possible. It is well known that the vehicle can affect skin permeation, and the resulting difference in the epidermal disposition kinetics parameters could be further investigated. For cinnamic aldehyde, previously considered with four different vehicles (Pendlington *et al.*, 2008), the present analysis indicates that changing the vehicle leads to greater variation in C_{max} than in AUC values (in either epidermis or dermis). In order to use the methods presented here in consumer safety risk assessment, the effects of vehicles and dose scenarios that are more representative of consumer use on the epidermal disposition kinetics would require consideration.

SUPPLEMENTARY DATA

The supplementary data are available online at http://toxsci.oxfordjournals.org/. The supplementary data files are the data spreadsheets from the time course skin permeation experiments. There is one spreadsheet for each chemical and concentration tested, with file names given in table 3. Where two concentrations were tested for the same chemical, the online titles with the lower "Test Prep" number correspond to the lower concentration. For cinnamic aldehyde, the online titles and vehicles tested were: Test Prep 1, propylene glycol; Test Prep 2, acetone:olive oil (4:1, v:v, AOO); Test Prep 3, aqueous ethanol (1:1, v:v); Test Prep 4, ethanol. For MPT, the "Expt 1" file corresponds to acetone:olive oil (4:1, v:v) containing 5% (v:v) ethanol, and the 'Expt 2' file to acetone:olive oil (4:1, v:v) containing 5% (v:v) tetrahydrofuran. Each spreadsheet contains six sets of worksheets, one set for each terminal sampling time point, labelled accordingly by the names on the worksheet tabs. For a given time point, the worksheets have one of two formats depending on whether the experiments were performed at Unilever SEAC or Charles River. In the first case, there is one worksheet containing the data for each sample, and they are all summarised on the '14C Recovery' sheet in terms of percentage of applied dose, except for the individual tape strip data on the "TAPE" worksheet. In the second case, all data are contained on the "Raw Data" worksheet, with the first block of data in percentage of applied dose and later blocks in $\mu g/cm^2$ equivalent; the same data are also included with additional labelling on the "% Applied Dose" and "μg equiv.cm2" worksheets respectively.

ACKNOWLEDGMENTS

This work is part of Unilever's ongoing research to deliver novel ways of assuring consumer safety. We wish to thank Juliette Pickles for helpful comments on the manuscript.

REFERENCES

Aleksic, M., Thain, E., Roger, D., Saib, O., Davies, M., Li, J., Aptula, A., and Zazzeroni, R. (2009). Reactivity profiling: covalent modification of single

nucleophile peptides for skin sensitization risk assessment. *Toxicol. Sci.* **108,** 401–411.

Basketter, D., Pease, C., Kasting, G., Kimber, I., Casati, S., Cronin, M., Diembeck, W., Gerberick, F., Hadgraft, J., Hartung, T., *et al.* (2007). Skin sensitisation and epidermal disposition: the relevance of epidermal disposition for sensitisation hazard identification and risk assessment. The report and recommendations of ECVAM workshop 59. *Altern. Lab. Anim.* **35,** 137–154.

Chen, L. J., Lian, G. P., and Han, L. J. (2008). Use of "bricks and mortar" model to predict transdermal permeation: model development and initial validation. *Ind. Eng. Chem. Res.* **47,** 6465–6472.

Chilcott, R. P., Barai, N., Beezer, A. E., Brain, S. I., Brown, M. B., Bunge, A. L., Burgess, S. E., Cross, S., Dalton, C. H., Dias, M., *et al.* (2005). Inter- and intralaboratory variation of in vitro diffusion cell measurements: an international multicenter study using quasi-standardized methods and materials. *J. Pharm. Sci.* **94,** 632–638.

European Union (EU) (2003). Directive 2003/15/EC of the European Parliament and of the Council of 27 February 2003 amending Council Directive 76/768/EEC on the approximation of the laws of the Member States relating to cosmetic products. *Off. J. Eur. Union* **L66,** 26–35.

Fentem, J., Chamberlain, M., and Sangster, B. (2004). The feasibility of replacing animal testing for assessing consumer safety: a suggested future direction. *Altern. Lab. Anim.* **32,** 617–623.

Fukunaga, A., Khaskhely, N. M., Sreevidya, C. S., Byrne, S. N., and Ullrich, S. E. (2008). Dermal dendritic cells, and not Langerhans cells, play an essential role in inducing an immune response. *J. Immunol.* **180,** 3057–3064.

Gerberick, G. F., Vassallo, J. D., Foertsch, L. M., Price, B. B., Chaney, J. G., and Lepoittevin, J. P. (2007). Quantification of chemical peptide reactivity for screening contact allergens: a classification tree model approach. *Toxicol. Sci.* **97,** 417–427.

Griffiths, C. E. M., Dearman, R. J., Cumberbatch, M., and Kimber, I. (2005). Cytokines and Langerhans cell mobilisation in mouse and man. *Cytokine* **32,** 67–70.

Jowsey, I. R., Basketter, D. A., Westmoreland, C., and Kimber, I. (2006). A future approach to measuring relative skin sensitising potency: a proposal. *J. Appl. Toxicol.* **26,** 341–350.

Kass, R. E., and Raftery, A. E. (1995). Bayes factors. *J. Am. Stat. Assoc.* **90,** 773–795.

Kasting, G. B., Miller, M. A., and Bhatt, V. D. (2008). A spreadsheet-based method for estimating the skin disposition of volatile compounds: application to N, N-diethyl-m-toluamide (DEET). *J. Occup. Environ. Hyg.* **5,** 633–644.

Kimber, I., Cumberbatch, M., and Dearman, R. J. (2009). Langerhans cell migration: not necessarily always at the center of the skin sensitization universe. *J. Invest. Dermatol.* **129,** 1852–1853.

Maxwell, G., Aleksic, M., Aptula, A., Carmichael, P., Fentem, J., Gilmour, N., MacKay, C., Pease, C., Pendlington, R., Reynolds, F., *et al.* (2008). Assuring consumer safety without animal testing: a feasibility case study for skin sensitisation. *Altern. Lab. Anim.* **36,** 557–568.

McCarley, K. D., and Bunge, A. L. (2001). Pharmacokinetic models of dermal absorption. *J. Pharm. Sci.* **90,** 1699–1719.

Natsch, A., Emter, R., and Ellis, G. (2009). Filling the concept with data: integrating data from different in vitro and in silico assays on skin sensitizers to explore the battery approach for animal-free skin sensitization testing. *Toxicol. Sci.* **107,** 106–121.

Nitsche, J. M., and Kasting, G. B. (2008). Biophysical models for skin transport and absorption. In *Dermal Absorption and Toxicity Assessment* (M. S. Roberts and K. A. Walters, Eds.), pp. 251–269. Informa Healthcare USA, New York.

Organization for Economic Cooperation and Development (OECD). (2002). *Guideline for the Testing of Chemicals—Guideline 429: Skin Sensitisation: Local Lymph Node Assay*. Organization for Economic Cooperation and Development, Paris.

Organization for Economic Cooperation and Development (OECD). (2004a). Guidance Document for the Conduct of Skin Absorption Studies. *Series on Testing and Assessment No. 28*. Organization for Economic Cooperation and Development, Environment Directorate, OECD Environmental Health and Safety Publications, Paris.

Organization for Economic Cooperation and Development (OECD). (2004b). *Guideline for Testing of Chemicals—Guideline 428: Skin Absorption:* In Vitro *Method.* Organization for Economic Cooperation and Development, Paris.

Pendlington, R. U., Minter, H. J., Stupart, L., MacKay, C., Roper, C. S., Sanders, D. J., and Pease, C. K. (2008). Development of a modified in vitro skin absorption method to study the epidermal/dermal disposition of a contact allergen in human skin. *Cutan. Ocul. Toxicol.* **27,** 283–294.

Potts, R. O., and Guy, R. H. (1992). Predicting skin permeability. *Pharm. Res.* **9,** 663–669.

Roberts, D. W., Aptula, A. O., Patlewicz, G., and Pease, C. (2008). Chemical reactivity indices and mechanism-based read-across for non-animal based assessment of skin sensitisation potential. *J. Appl. Toxicol.* **28,** 443–454.

Roberts, D. W., Patlewicz, G., Kern, P. S., Gerberick, F., Kimber, I., Dearman, R. J., Ryan, C. A., Basketter, D. A., and Aptula, A. O. (2007). Mechanistic applicability domain classification of a local lymph node assay dataset for skin sensitization. *Chem. Res. Toxicol.* **20,** 1019–1030.

Saiyasombati, P., and Kasting, G. B. (2003). Two-stage kinetic analysis of fragrance evaporation and absorption from skin. *Int. J. Cosmet. Sci.* **25,** 235–243.

Schultz, T. W., Rogers, K., and Aptula, A. O. (2009). Read-across to rank skin sensitization potential: subcategories for the Michael acceptor domain. *Contact Dermatitis* **60,** 21–31.

Schwarz, G. (1978). Estimating dimension of a model. *Ann. Stat.* **6,** 461–464.